

An ab Initio Investigation of the Reactions of 1,1- and 1,2-Dichloroethane with Hydroxyl Radical

Asit K. Chandra

Research Institute of Innovative Technology for the Earth, c/o National Institute of Materials and Chemical Research, 1-1 Higashi, Tsukuba Science City, Ibaraki 305-8565, Japan

Tadafumi Uchimaru*

Department of Physical Chemistry, National Institute of Materials and Chemical Research, 1-1 Higashi, Tsukuba Science City, Ibaraki 305-8565, Japan

Received: May 19, 1999; In Final Form: September 23, 1999

The hydrogen abstraction reactions by OH radical from 1,1-dichloroethane and 1,2-dichloroethane have been investigated by ab initio molecular orbital theory. Optimized geometries and harmonic vibrational frequencies have been calculated for all reactants, transition structures, and products at the (U)HF/6-311G(d,p) and (U)MP2=full/6-311G(d,p) levels of theory. Single point QCISD(T)/6-311G(d,p)/(U)MP2=full/6-311G(d,p) calculations have also been carried out for the inclusion of higher order electron correlation. Three distinct transition structures have been located for the $\text{H}_3\text{C}-\text{CHCl}_2 + \text{OH}$ reaction (one for α -abstraction and two for β -abstraction). Four transition structures have been located for the reaction $\text{ClH}_2\text{C}-\text{CH}_2\text{Cl} + \text{OH}$. The calculated barrier heights, reaction enthalpies, and change in entropy are found to be in good agreement with available experimental values. In addition, the rate constants calculated by using the transition state theory are found to be in good agreement with the experimental results. Non-Arrhenius behavior of the rate constants arises from the tunneling effects and availability of multiple reaction channels.

Introduction

The chlorofluorocarbons (CFCs) are known to be responsible for the depletion of ozone layer in the stratosphere and the greenhouse effects.¹ The design of ecofriendly compounds for the replacements of CFCs is thus an important area of research. Partially halogenated hydrocarbons (HCFCs) with shorter tropospheric lifetime and appropriate thermochemical properties may serve as suitable replacements to the CFCs as refrigerants, propellants, solvents, etc.² The hydrogen abstraction reaction with hydroxyl (OH) radical is the main channel of tropospheric degradation for the HCFCs.³ Considerable attention has thus been paid to this reaction and it has been the subject of theoretical investigations by using high level ab initio quantum chemical methods.^{4–16}

In the present work, ab initio molecular orbital calculations have been carried out for the following hydrogen abstraction reactions between dichloroethanes (DCEs) and OH radical:



Reactions with OH radical are the major degradation processes of these hydrocarbons under both atmospheric and combustion conditions.¹⁷ Thus a fundamental understanding of the chemical reactions between OH radical and chlorinated

hydrocarbons is very important. Experimental data on the title reactions are quite scarce,^{18–20} and to the best of our knowledge there have been no theoretical calculations on these systems. Moreover, in the case of 1,1-dichloroethane (1,1-DCE), the hydrogen atoms in α - (the Cl-bearing carbon atom) and β -positions (unsubstituted carbon atom) are not equivalent and thus several modes of hydrogen abstraction are possible. More than one reaction path can also be possible for hydrogen abstraction from 1,2-DCE. Taylor et al¹⁹ observed significant non-Arrhenius behavior in the reaction of 1,2-DCE and OH radical and suggested that non-Arrhenius behavior might be due to the availability of multiple reaction channels. It is difficult to know from the experiment which hydrogen atom is abstracted. Theoretical investigations are thus needed for the better understanding of these reactions. Furthermore, high level ab initio calculations can be applied to these systems.

We have located several transition states for each of the reactions R1, R2, and R3. We will present the structures, energetics, and vibrational frequencies of each stationary point, i.e., the reactants, transition states (TSs), and products. We applied high level ab initio quantum chemical methods, up to QCISD(T), to evaluate the energy of each stationary point. Each reaction path will be described separately in the Results and Discussion section.

Computational Methods

Computational level was chosen based on the experience of earlier studies on hydrogen abstraction reactions between OH radical and halocarbons.^{11,12} The geometries of the closed shell species (CH_3CHCl_2 , $\text{CH}_2\text{ClCH}_2\text{Cl}$, H_2O) were optimized at the restricted Hartree–Fock (HF) level, whereas unrestricted Har-

* To whom correspondence should be addressed. Email: t_uchimaru@home.nimc.go.jp. Tel: +81-298-54-4522. Fax: +81-298-54-4487.

TABLE 1: Geometrical Parameters Optimized at the (U)HF/6-311G(d,p) and (U)MP2=full/6-311G(d,p) Levels for the Reactants and Products Involved in the Reaction of 1,1-Dichloroethane with OH Radical (reactions R1 and R2 described in Text)^a

parameters	(U)HF	(U)MP2	exptl ^b	parameters	(U)HF	(U)MP2
CH ₃ CHCl ₂				CH ₂ CHCl ₂		
r(C1-C2)	1.5125	1.5103	1.540	r(C1-C2)	1.4793	1.4726
r(C2-Cl)	1.7847	1.7772	1.766	r(C2-Cl1)	1.7806	1.7759
r(C2-H)	1.0742	1.0874		r(C2-C12)	1.8042	1.7998
r(C1-H)	1.0837	1.0918		r(C1-H[av])	1.0737	1.0811
r(C1-H')	1.0823	1.0908		θ(C1-C2-Cl1)	112.4	112.0
θ(C1-C2-Cl)	110.9	110.4	111.0	θ(C1-C2-Cl2)	111.4	111.0
θ(C1-C2-H)	112.3	111.8		θ(C1-C2-H)	110.8	110.3
θ(C2-C1-H)	109.4	109.7		θ(C2-C1-H[av])	118.8	119.1
θ(C2-C1-H')	110.6	110.1		θ(H-C2-C1-H')	35.0	30.0
φ(Cl1-C2-C1-H)	58.8	58.3		θ(H'-C2-C1-H')	162.0	165.0
φ(Cl2-C1-C2-Cl1)	122.9	123.1		CH ₃ CCl ₂ [*]		
hydroxyl radical				r(C1-C2)	1.4950	1.4891
r(O-H)	0.9512	0.9657	0.9706	r(C2-Cl)	1.7313	1.7190
H ₂ O				r(C1-H)	1.0830	1.0913
r(O-H)	0.9411	0.9572	0.9576	r(C1-H')	1.0878	1.0975
θ(H-O-H)	105.4	102.5	104.5	θ(C1-C2-Cl)	117.6	117.2
				θ(C2-C1-H)	109.6	109.9
				θ(C2-C1-H')	110.9	110.9
				φ(Cl1-C1-C2-Cl2)	144.8	145.0
				φ(Cl1-C2-C1-H')	47.8	47.4

^a Bond lengths in angstroms, angles in degrees. ^b From ref 42.

tree-Fock (UHF) theory was used for the open shell species (OH, TS, and dichloroethyl radicals). Each structure was characterized by performing harmonic vibrational frequency calculation at the same level of theory. Subsequently, starting from the optimized geometries at the HF/UHF level, the geometries of all the reactants, TSs and products were optimized further at the second order Moller-Plesset level, MP2 and UMP2, including all electrons in correlation. Vibrational frequencies were also calculated at the (U)MP2 level for characterizing the geometries obtained from optimization. Finally, single-point QCISD(T) calculations were performed on the (U)MP2 optimized geometries to include higher order electron correlation effect. It may be worthwhile to point out that the density functional theory (DFT) does not produce good results for the hydrogen abstraction reactions. We initially applied B3LYP DFT-method for the present problem. But the results obtained were rather poor and the calculated barrier heights were found to be negative, which is not in accord with the experimental observations.^{18,19} Intrinsic reaction coordinate (IRC) calculations were performed at the UMP2=full level to confirm that each TS was located along the reaction coordinate for hydrogen abstraction. The IRC calculations were performed for eight steps (step length = 0.01 au) in the forward direction starting from the TS. At the final step, the breaking C-H bond length becomes nearly 1.6 Å, whereas the forming O-H bond length becomes like a O-H bond in water (0.96 Å). As the hydrogen atom being abstracted goes off, the geometrical parameters of the haloethyl radical residue slowly approach to the values found for the isolated radical. These show that the TS leads to haloethyl radical and H₂O molecule. However, in majority of the cases, there were convergence problems in the IRC calculations after a few steps towards the reactants side. It should be pointed out that the formation of pre-reaction or post-reaction van der Waals complexes are possible.¹⁴ However, in the present study a detailed analysis of the IRC path has not been made and such possibilities are not discussed further. Thermal corrections to the QCISD(T) energies were made by using the vibrational frequencies at the (U)MP2 level. (U)HF and (U)MP2 vibrational frequencies were scaled by factors of 0.9051 and 0.9496,²¹ respectively, for estimating zero-point vibrational energies (ZPVEs) and the thermal corrections to the energies. Standard 6-311G(d,p) basis set was employed for all

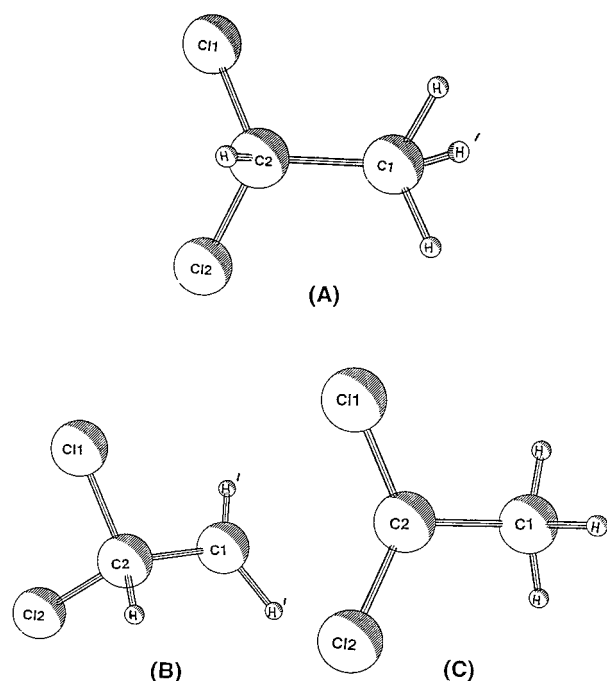


Figure 1. Schematic structures of 1,1-dichloroethane (A) and two product radicals, CH₂CHCl₂ (B), and CH₃CCl₂ (C). Geometries were optimized at the (U)HF and (U)MP2 levels with the 6-311G(d,p) basis set. Overall structures are essentially the same at both the levels (see Table 1).

the calculations. All calculations were performed by using the Gaussian-94 suite of programs²² and on a Silicon Graphics Origin 200 workstation.

It is well-known that supermolecular calculations with an incomplete basis set suffer from the basis set superposition error (BSSE). The effect of BSSE on the potential energy surface and the procedure for estimating BSSE have been discussed extensively in the literature for the weakly bound complexes.^{23,24} However, little attention has so far been paid to the problem of BSSE in the potential energy surface of a reaction. Scheiner and co-workers analyzed this problem for the proton transfer reaction.²⁵ Very recently, Sekusak and Sabljic evaluated the

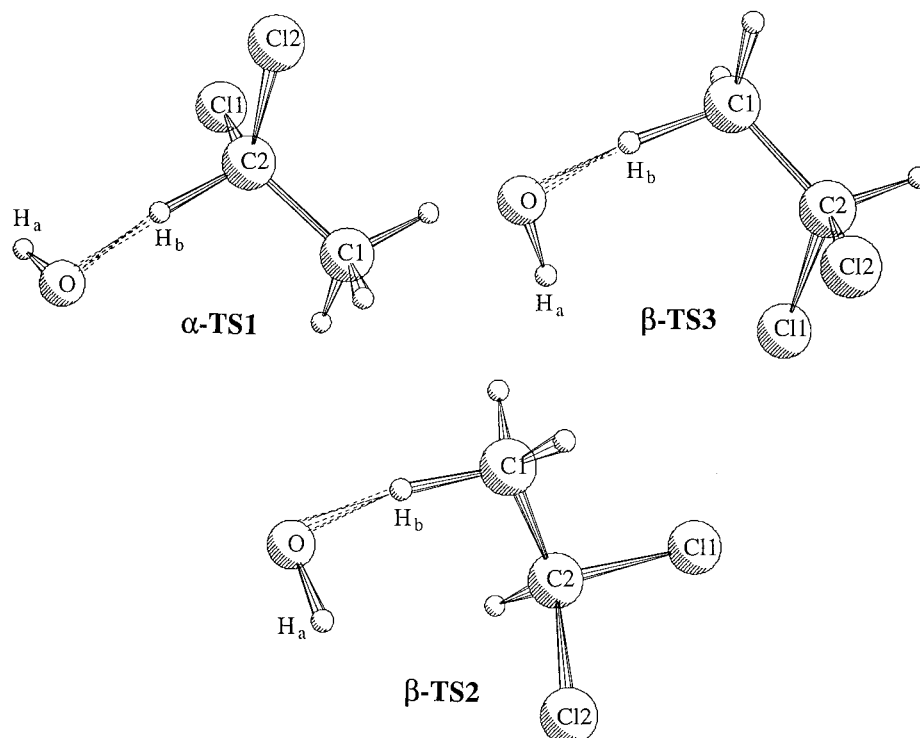


Figure 2. Transition-state geometries for the hydrogen abstraction reactions from 1,1-dichloroethane as obtained from the UMP2=full/6-311G(d,p) calculations.

effect of BSSE on the calculated activation energies for the hydrogen abstraction reactions between haloethanes and OH radical.²⁶ They observed that the uncorrected results were always more close to the experiment than the BSSE corrected results and advised that one should use BSSE uncorrected results obtained from a reasonably large basis set. Moreover, BSSE correction for the potential energy surface of a reaction has some other technical problems which has been discussed by Scheiner et al.²⁵ In the present work, the BSSE for the calculated barrier heights were evaluated by using the counterpoise (CP) method of Boys and Bernardi²⁷ and are presented in the next section. However, due to the points mentioned above and the lack of a well settled method to eliminate this error, the BSSE corrected results were not used for the kinetic calculations.

Results and Discussion

1. Structures and Vibrational Frequencies. A. 1,1-Dichloroethane (Reactions R1 and R2). Hydrogen atom can be abstracted from the Cl-bearing carbon atom (reaction R1) as well as from the unsubstituted carbon atom (reaction R2). Both the reactions were studied and the corresponding TSs were located. Table 1 presents the optimized structures obtained at the (U)HF and (U)MP2 levels for the reactants and products of reactions R1 and R2. Available experimental values are also given for comparison. The geometries optimized at the (U)HF and at the (U)MP2 level are not much different except for the C–H and O–H bond lengths. These bond lengths are always found to be longer at the MP2 level. MP2 results are in reasonable agreement with the available experimental results for 1,1-DCE, OH radical, and water molecule.

1,1-DCE has C_s symmetry (Figure 1A) and contains one α -hydrogen atom (bonded to the Cl-bearing carbon atom) and three β -hydrogen atoms (bonded to the unsubstituted carbon atom). Three β -hydrogens are not equivalent; one is (H' in Figure 1) different from the other two. Accordingly, three TSs, one (α -TS1) for α -hydrogen abstraction in R1 and two (β -TS2

TABLE 2: Key Geometrical Parameters Optimized at the (U)HF/6-311G(d,p) and (U)MP2=full/6-311G(d,p) Levels for the Three Transition Structures for the Reactions R1 and R2^a

parameter	UHF	UMP2	parameter	UHF	UMP2
α -TS1					
$r(\text{C2-Hb})$	1.283	1.178	$r(\text{O-Hb})$	1.199	1.324
$r(\text{Ha-Clx})$	3.33	3.08	$\theta(\text{C1-C2-Hb})$	105.6	107.5
$\theta(\text{C2-Hb-O})$	177.1	168.1	$\theta(\text{Hb-O-Ha})$	99.2	96.1
β -TS2					
$r(\text{C1-Hb})$	1.302	1.201	$r(\text{O-Hb})$	1.193	1.288
$r(\text{Ha-Clx})$	3.11	2.81	$\theta(\text{C2-C1-Hb})$	106.9	107.5
$\theta(\text{C1-Hb-O})$	173.1	164.8	$\theta(\text{Hb-O-Ha})$	99.8	96.7
β -TS3					
$r(\text{C1-Hb})$	1.310	1.207	$r(\text{O-Hb})$	1.185	1.272
$r(\text{Ha-Clx})$	3.07	2.81	$\theta(\text{C2-C1-Hb})$	110.4	109.4
$\theta(\text{C1-Hb-O})$	174.7	167.6	$\theta(\text{Hb-O-Ha})$	100.1	97.4

^a Bond lengths and angles are in angstroms and degrees, respectively.

and β -TS3) for β -hydrogen abstraction in R2, have been located. Figure 2 shows the pictures of these three TSs. In β -TS2, the β -hydrogen atom being abstracted is *trans* to a Cl-atom, whereas in β -TS3, the abstracted β -hydrogen atom is *gauche* to the Cl-atoms. The structural differences in the TSs introduce a change in intramolecular interactions. Table 2 presents key structural parameters for the TSs and the distance between the hydroxyl hydrogen and the closest Cl-atom ($H_a\text{-Cl}_x$). This distance provides an indication of the degree of intramolecular hydrogen bonding present in the TSs. Theoretical evidences for the $\text{H}\cdots\text{F}$ and $\text{H}\cdots\text{Cl}$ hydrogen bonding in TSs for hydrogen abstraction from fluorocarbon have been reported previously.^{11,3,28} Hydrogen bonding can occur when the distance between a hydrogen atom and an electronegative donor atom is significantly less than the sum of their van der Waals radii. These values are 1.2 and 1.8 Å for hydrogen and chlorine atoms, respectively.²⁹ Thus a $\text{H}\cdots\text{Cl}$ distance of significantly less than 3.0 Å can be taken as an indication of the presence of intramolecular hydrogen bonding

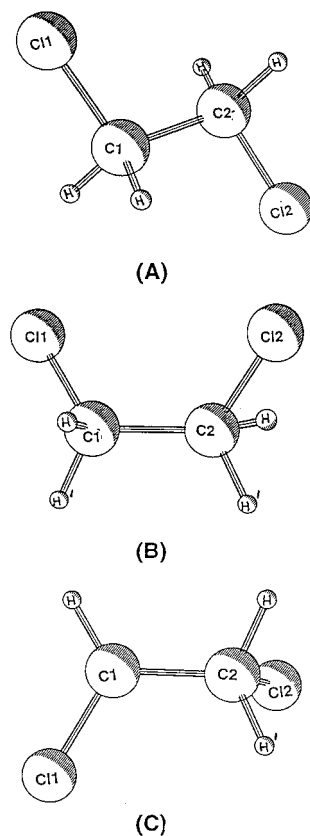


Figure 3. Schematic structures of 1,2-dichloroethane [*trans* (A), *gauche* (B)] and the product radical, CH_2ClCHCl (C). Geometries were optimized at the (U)HF and (U)MP2 levels with the 6-311G(d,p) basis set. Overall structures are essentially the same at both the levels (see Table 3).

in the TS. Table 2 shows that in β -TS2 and β -TS3 the closest $\text{H}\cdots\text{Cl}$ distance at UMP2 level is 2.81 Å, which is significantly shorter than the sum of their van der Waals radii: the incoming OH radical is oriented to take advantage of an intramolecular hydrogen bond. The $\text{H}\cdots\text{Cl}$ distances are found to be larger than the sum of van der Waals radii of hydrogen and chlorine atoms at the UHF level of theory. This is obviously due to the lack of electron correlation at this level and thus cannot take into account the effect of dispersion forces.

According to Hammond's postulate,³⁰ the TS should be more reactant like for an exoergic reaction. Since hydrogen abstraction

from halocarbons by OH radical is generally exoergic (see the results discussed later), it can be expected that TSs for the reactions R1 and R2 would be reactant like. The geometrical parameters for the TSs, except for the breaking C–H bond length, do not change significantly from those at the isolated reactants. The above observations can be put in a more general perspective by defining a quantity⁶

$$R_b = \frac{(r_b - r_{b,\text{eq}})/r_{b,\text{eq}}}{(r_b - r_{b,\text{eq}})/r_{b,\text{eq}} + (r_f - r_{f,\text{eq}})/r_{f,\text{eq}}}$$

where r_b and $r_{b,\text{eq}}$ are the breaking bond length (C–H in the present case) in the TS and in the reactant, respectively, whereas r_f and $r_{f,\text{eq}}$ are the forming bond length ($\text{O}\cdots\text{H}$ in the present case) in the TS and in the equilibrium structure of the product, respectively. Hammond's postulate suggests that the value of R_b becomes smaller as the exoergic of a reaction increases. The R_b values calculated at the HF/MP2 level are 0.41/0.18, 0.43/0.22, and 0.45/0.25 for the α -TS1, β -TS2 and β -TS3, respectively. All the R_b values are less than 0.5, which indicates early TSs. MP2 R_b values are consistently lower than the HF values, signifying that the MP2 TSs are further out in the reaction channel. The breaking C–H bond in the TSs are found to be longer (by almost 0.1 Å) at the UHF level than those at the UMP2 level. The opposite trend has been observed for the forming $\text{O}\cdots\text{H}$ bond. Similar observations were made for the hydrogen atom abstraction reactions from methane,^{5,6,31} ethane,¹¹ fluoromethanes,^{15,16} fluoroethanes,¹¹ and chloroethane.²⁸ Compared to the UHF results, the C–H \cdots O angle is always more bend at the UMP2 level. For example, the UHF and UMP2 values for the C–H \cdots O angle in α -TS1 are 177.1 and 168.1°, respectively.

Harmonic vibrational frequencies of 1,1-DCE and all other stationary involved in reactions R1 and R2 are given in Tables S1 and S2 as Supporting Information. The imaginary frequencies in the TS correspond to the coupling of C–H_b and O–H_b (see Figure 2) stretching vibrational modes, i.e., transfer of hydrogen from DCE to the OH radical. As expected, the (U)MP2 frequencies in general are lower than the corresponding (U)HF values. In particular, the imaginary frequencies for all the TSs are almost 40% lower at the UMP2 level compared to those at the UHF level. This is consistent to the fact that TSs at the UMP2 level are lying further out in the entrance channel. The indication of weak hydrogen bonding in β -TS2 and β -TS3 can be observed from the frequencies of the normal mode vibration

TABLE 3: Geometrical Parameters Optimized at the (U)HF/6-311G(d,p) and (U)MP2=full/6-311G(d,p) Levels for Reactants and Products Involved in the Reaction of 1,2-Dichloroethane with OH Radical (Reactions R3 Described in Text)

parameter	HF	MP2	expt ^b	parameter	UHF	UMP2
$\text{CH}_2\text{ClCH}_2\text{Cl}$ (<i>trans</i>)				$\text{CH}_2\text{ClCHCl}^\bullet$		
$r(\text{C1}-\text{C2})$	1.5139	1.5127	1.531	$r(\text{C1}-\text{C2})$	1.4778	1.4713
$r(\text{C}-\text{Cl})$	1.7955	1.7801	1.790	$r(\text{C1}-\text{Cl1})$	1.7230	1.7020
$r(\text{C}-\text{H})$	1.0777	1.0889	1.11	$r(\text{C2}-\text{Cl2})$	1.8174	1.8084
$\theta(\text{C}-\text{C}-\text{Cl})$	109.4	109.3	109.0	$r(\text{C1}-\text{H})$	1.0718	1.0808
$\theta(\text{C}-\text{C}-\text{H})$	111.6	110.8	113.0	$r(\text{C2}-\text{H}')$	1.0785	1.0896
$\theta(\text{Cl}-\text{C}-\text{C}-\text{Cl})$	180.0	180.0	180.0	$r(\text{C2}-\text{H})$	1.0772	1.0889
$\text{CH}_2\text{ClCH}_2\text{Cl}$ (<i>gauche</i>)				$\theta(\text{C2}-\text{C1}-\text{H})$	121.6	121.5
$r(\text{C1}-\text{C2})$	1.5117	1.5117		$\theta(\text{C2}-\text{C1}-\text{Cl1})$	119.4	119.3
$r(\text{C}-\text{Cl})$	1.7900	1.7760		$\theta(\text{C1}-\text{C2}-\text{H}')$	110.3	110.1
$r(\text{C}-\text{H}')$	1.0804	1.0915		$\theta(\text{C1}-\text{C2}-\text{Cl2})$	112.0	111.9
$r(\text{C}-\text{H})$	1.0781	1.0895		$\theta(\text{C1}-\text{C2}-\text{H})$	112.0	111.5
$\theta(\text{C}-\text{C}-\text{Cl})$	112.7	112.2		$\phi(\text{Cl1}-\text{C2}-\text{C1}-\text{H})$	204.8	203.3
$\theta(\text{C}-\text{C}-\text{H}')$	109.1	108.9		$\phi(\text{Cl1}-\text{C1}-\text{C2}-\text{Cl2})$	81.6	79.5
$\theta(\text{C}-\text{C}-\text{H})$	111.5	110.7				
$\theta(\text{Cl}-\text{C}-\text{C}-\text{Cl})$	70.5	68.0				

^a Bond lengths and angles are in angstroms and degrees, respectively. ^b Reference 42.

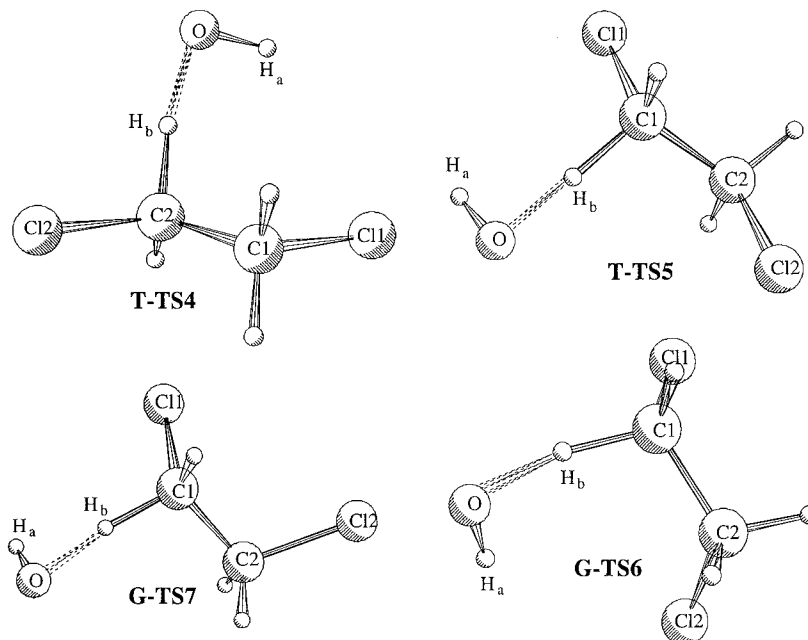


Figure 4. Transition-state geometries for the hydrogen abstraction reactions from 1,2-dichloroethane as obtained from the UMP2=full/6-311G(d,p) calculations.

associated with the torsional motion of OH in the TSs. The (U)MP2 frequencies of this mode for β -TS2 and β -TS3 are 229 and 165 cm^{-1} , respectively, whereas the corresponding frequency amounts to only 70 cm^{-1} for the α -TS1. This difference is clearly due to the presence of weak hydrogen bonding between the hydroxyl hydrogen and chlorine atom in β -TS2 and β -TS3. Accordingly, the entropies of β -TS2 (84.9 cal/mol K) and β -TS3 (85.3 cal/mol K) at the UMP2 level are lower than that of the α -TS1 (86.7 cal/mol K).

B. 1,2-Dichloroethane (Reaction R3). 1,2-DCE has two stable conformers, *trans* and *gauche* (see Figure 3). *Trans* conformer is known to be lower in energy.³² Table 3 presents the geometrical parameters of the two conformers of 1,2-DCE and 1,2-dichloroethyl radical optimized at the (U)HF and (U)MP2 level. All four hydrogen atoms are equivalent in *trans* 1,2-DCE (C_{2h} symmetry), whereas in *gauche* form (C_2 symmetry) two hydrogen atoms (one in each carbon atom) can be distinguished from the other two. Structural parameters obtained from the (U)HF and (U)MP2 calculations are found to be close to each other. In the 1,2-dichloroethyl radical the C1–C11 (see Figure 3C) bond length is about 0.1 Å shorter than the C2–C12 distance. Available experimental results are also included in the table for comparison. The MP2 results are found to be in reasonable agreement with the experimental values. The C–Cl distances in *trans* and *gauche* 1,2-DCE are found to be longer than that in 1,1-DCE.

Four TSs have been located for the hydrogen abstraction reaction between 1,2-DCE and OH radical (R3). Figure 4 displays the structures of these four TSs for the reaction R3 and Table 4 presents the optimized geometrical parameters of the four TSs. In two TSs, 1,2-DCE is in *trans* conformation (T-TS4 and T-TS5), whereas it is in *gauche* conformation in the other two TSs (G-TS6 and G-TS7). In one of the two TSs for each conformer, the hydroxyl hydrogen forms a hydrogen bond with a Cl-atom. In T-TS4 and G-TS6, the distances between the hydroxyl hydrogen and the closest β -chlorine atom at the UMP2 level are 2.81 and 2.76 Å, respectively, which are considerably shorter than the sum of van der Waals radii of the two atoms. In T-TS5 and G-TS7, the distances between the hydroxyl hydrogen and the α -chlorine atoms are longer than

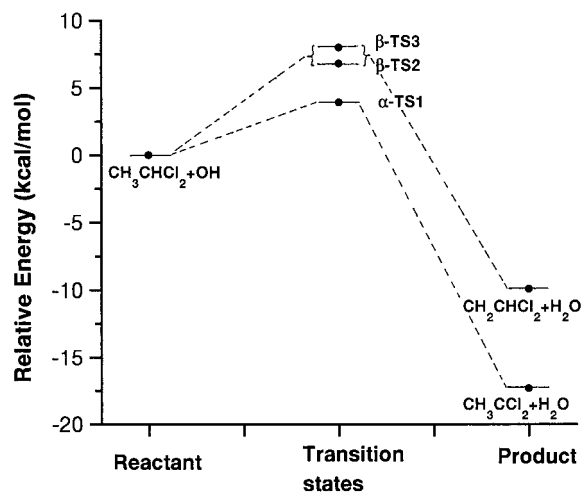


Figure 5. Schematic diagram of the QCISD(T)/6-311G(d,p) energy profiles for hydrogen abstraction by OH radical from 1,1-dichloroethane.

the sum of their van der Waals radii. The weak hydrogen bonding interaction gives additional stability to the T-TS4 and G-TS6 in comparison to T-TS5 and G-TS7, respectively (see Table 6 and Figure 6). Once again, compared to the HF level, TSs at the MP2 level are found to be further out in the entrance channel. MP2 bond length for the breaking C–H bond is significantly shorter than the HF value, whereas the forming O...H bond is longer at the MP2 level than that at the HF-level. The R_b values for the T-TS4, T-TS5, G-TS6, and G-TS7 calculated using geometrical parameters at the HF/MP2 level are 0.44/0.20, 0.44/0.22, 0.43/0.17, and 0.42/0.21, respectively. Thus, TSs are found to be reactant like, consistent with Hammond's postulate for an exoergic reaction. The MP2 R_b values are much smaller than the HF values, indicating that the MP2 TSs are more reactant like than the HF TSs.

Calculated and experimental vibrational frequencies of 1,2-DCE are listed in Table 5. Those for the four TSs and 1,2-dichloroethyl radical are given in Table S3 as Supporting Information. In accord with the general trend, HF frequencies are higher than those at the MP2 level. Calculated frequencies

TABLE 4: Key Geometrical Parameters Optimized at the (U)HF/6-311G(d,p) and (U)MP2=full/6-311G(d,p) Levels for the Four Transition Structures for the Reactions R3^a

parameter	UHF	UMP2	parameter	UHF	UMP2
T-TS4					
$r(\text{C2-Hb})$	1.298	1.191	$r(\text{O-Hb})$	1.189	1.299
$r(\text{Ha-Clx})$	3.05	2.81	$\theta(\text{C1-C2-Hb})$	108.0	108.1
$\theta(\text{C2-Hb-O})$	172.3	165.8	$\theta(\text{Hb-O-Ha})$	100.5	97.6
T-TS5					
$r(\text{C1-Hb})$	1.299	1.194	$r(\text{O-Hb})$	1.189	1.296
$r(\text{Ha-Clx})$	3.10	2.97	$\theta(\text{C2-C1-Hb})$	107.2	107.0
$\theta(\text{C1-Hb-O})$	172.0	165.0	$\theta(\text{Hb-O-Ha})$	99.4	96.0
G-TS6					
$r(\text{C1-Hb})$	1.297	1.192	$r(\text{O-Hb})$	1.190	1.301
$r(\text{Ha-Clx})$	3.04	2.76	$\theta(\text{C2-C1-Hb})$	108.7	108.9
$\theta(\text{C1-Hb-O})$	171.3	163.3	$\theta(\text{Hb-O-Ha})$	99.6	96.5
G-TS7					
$r(\text{C1-Hb})$	1.291	1.188	$r(\text{O-Hb})$	1.202	1.317
$r(\text{Ha-Clx})$	3.21	3.08	$\theta(\text{C2-C1-Hb})$	103.8	105.0
$\theta(\text{C1-Hb-O})$	174.4	163.4	$\theta(\text{Hb-O-Ha})$	98.9	95.6

^a Bond lengths and angles are in angstroms and degrees, respectively.

TABLE 5: Unscaled Harmonic Vibrational Frequencies (in cm^{-1}) of *trans* and *gauche* 1,2-Dichloroethane

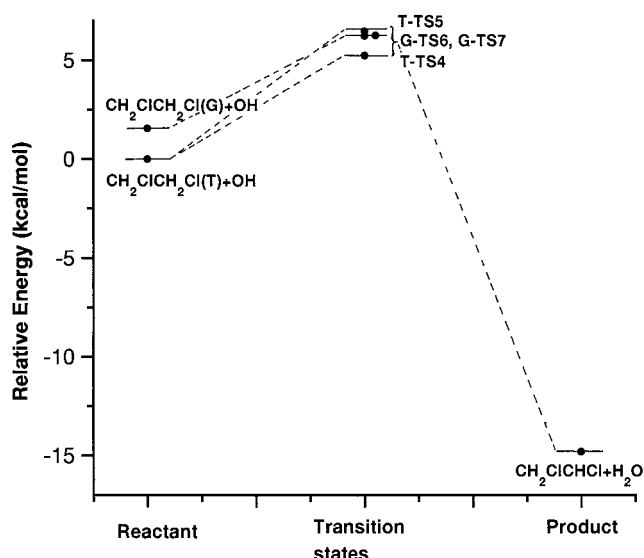
mode	trans			mode	gauche		
	HF	MP2	exptl ^a		HF	MP2	exptl ^a
torsion	127	136	123	torsion	123	130	125
CCCl deform ^b	233	223	222	CCCl deform	280	275	272
CCCl deform	322	316	300	CCCl deform	439	426	410
CCl stretch	769	788	728	CCl stretch	708	714	669
CH ₂ rock	827	798	773	CCl stretch	737	741	693
CCl stretch	833	831	754	CH ₂ rock	977	932	890
CH ₂ rock	1106	1055	989	CH ₂ rock	1034	998	948
CC stretch	1133	1106	1052	CC stretch	1131	1093	1027
CH ₂ twist	1254	1203	1123	CH ₂ twist	1270	1210	1146
CH ₂ wag	1383	1315	1232	CH ₂ twist	1345	1272	1207
CH ₂ twist	1410	1335	1264	CH ₂ wag	1449	1376	1292
CH ₂ wag	1478	1399	1304	CH ₂ wag	1479	1397	1315
CH ₂ sci	1612	1500	1445	CH ₂ sci	1593	1481	1433
CH ₂ sci	1618	1502	1461	CH ₂ sci	1601	1487	1436
CH ₂ sym str	3263	3146	2957	CH ₂ sym str	3240	3128	2957
CH ₂ sym str	3268	3153	2983	CH ₂ sym str	3252	3134	2957
CH ₂ anti str	3320	3209	3005	CH ₂ anti str	3307	3197	3005
CH ₂ anti str	3343	3230	3005	CH ₂ anti str	3319	3208	3005

^a Experimental results are taken from the ref 43. ^b deform = deformation. rock = rocking. wag = wagging. sci = scissoring. sym str = symmetric stretch. anti str = antistretch.

TABLE 6: Classical Barrier Heights (ΔE_0^\ddagger in kcal/mol) and Entropy of Activation (ΔS^\ddagger in $\text{cal mol}^{-1} \text{K}^{-1}$) Obtained from Various Levels of Theories with 6-311G(d,p) Basis Set

reaction	TS	ΔE_0^\ddagger			$\Delta S^\ddagger(298 \text{ K})$	
		HF	MP2(PMP2)	QCISD(T)	HF	MP2
R1	α -TS1	24.35	4.18(2.32)	2.03	-25.73	-27.66
R2	β -TS2	26.03	6.64(4.41)	5.24	-28.99	-29.48
	β -TS3	27.16	7.43(5.13)	6.21	-27.81	-29.04
R3	T-TS4	26.07	5.48(3.45)	3.63	-28.14	-28.47
	T-TS5	26.73	6.44(4.33)	4.69	-26.96	-26.93
	G-TS6	25.39	5.07(3.03)	3.17	-28.20	-28.77
	G-TS7	24.44	5.06(3.05)	3.07	-26.44	-26.78

at both the level are higher than those obtained from the experiment. This is due to the inadequacy of the theoretical method and the neglect of anharmonicity of potential energy surface. Discrepancy is found to be more in the case of stretching frequencies. Once again the imaginary frequencies at the UMP2 level are found to be substantially lower than the UHF values. This will have important effect on the tunneling correction to

**Figure 6.** Schematic diagram of the QCISD(T)/6-311G(d,p) energy profiles for hydrogen abstraction by OH radical from 1,2-dichloroethane.

the reaction rate, discussed recently by Petersson et al.¹⁶ Weak hydrogen bonding between the hydroxyl hydrogen atom and a chlorine atom bonded to the β -carbon makes the vibrational frequency associated with the internal rotational motion of OH radical in T-TS4 (227 cm^{-1}) and G-TS6 (238 cm^{-1}) significantly higher than that in T-TS5 (156 cm^{-1}) and G-TS7 (160 cm^{-1}), respectively. The indication of weak hydrogen bonding interaction can also be found from the entropies of the TSs. T-TS4 (85.35 cal/mol K) and G-TS6 (84.77 cal/mol K) have significantly lower entropies than those of T-TS5 (86.89 cal/mol K) and G-TS7 (86.76 cal/mol K), respectively.

2. Energetics and Reaction Enthalpies. *A. 1,1-Dichloroethane (Reactions R1 and R2).* Total energies, ZPVEs, and entropies of all species involved in the reactions R1 and R2 at different levels of theories are reported in Table S4 as Supporting Information. Figure 5 presents a graphical display of the same. Hydrogen abstraction from the α - and β -position results in two different products radical, CH_3CCl_2 and $\text{CH}_2\text{-CHCl}_2$, respectively. The former is found to be lower in energy by 7.20 kcal/mol at the UMP2 level of calculations. The energy difference amounts to 7.44 kcal/mol at the QCISD(T) level of theory. This difference in energy indicates a significant difference in C-H bond energies in the α and β positions. Due to lower C-H bond dissociation energy, the hydrogen abstraction from the α -position should have lower activation barrier. This is indeed the case, as evidenced from the energies of the three TSs. α -TS1 has much lower energy than the other two TSs related to β -hydrogen abstraction. It is known that, due to high spin contamination in the TS, the activation barrier may be overestimated by up to 10 kcal/mol when electron correlation are accounted by MP2 theory.³³ Energy obtained after spin projection is thus believed to produce more reliable activation barrier.²⁸ Energies obtained at the MP2 level after spin projections (PMP2) are also given in Table S1. Spin projection correction is much higher for the TS than that of the radical. This is because of more serious spin contamination in TSs than in OH and the product radicals. For example, the maximum $\langle S^2 \rangle$ value for the TSs amounts to 0.78, whereas the $\langle S^2 \rangle$ values do not exceed 0.765 for the product radicals.

Classical barrier heights (ΔE_0^\ddagger), entropy of activation (ΔS^\ddagger) for the reactions R1 and R2 are listed in Table 6. The classical barrier heights are calculated from the energy (including ZPVE) difference between the TS and the two reactants, 1,1-DCE and

TABLE 7: Basis Set Superposition Error (in kcal/mol) Calculated by the Counterpoise Method for Barrier Heights of Hydrogen Abstraction Reactions between Dichloroethane and OH Radical^a

TS	MP2	QCISD(T)
α -TS1	4.67	4.75
β -TS2	4.82	4.91
β -TS3	4.63	4.70
T-TS4	4.58	4.75
T-TS5	5.47	5.63
G-TS6	5.43	5.60
G-TS7	4.55	4.64

^a Calculations were performed with the 6-311G(d,p) basis set.

the OH radical. The barrier heights are found to be quite large at the HF level of theory. This is not surprising, since the inadequacy of HF level of theory for describing radical reactions was emphasized before.²⁸ Inclusion of electron correlation at the MP2 level of theory, brings down the barrier heights by almost 20 kcal/mol from those obtained at the HF level. As indicated earlier, the spin projection correction at the UMP2 level brings down the barrier heights further by more than 2 kcal/mol. The barrier heights obtained from our best calculations at the QCISD(T)/6-311G(d,p) level are significantly lower than those obtained from the (U)MP2 results. But, except for α -TS1, the QCISD(T)/6-311G(d,p) barrier heights are slightly higher than the corresponding PMP2 results. It is known that the calculated barrier heights cannot be directly compared to the experimental barrier heights (E_A).³⁴ However, from the results on other systems, it can be anticipated that comparison between E_A and ΔE_0^\ddagger for hydrogen transfer reactions is a reasonable approximation.^{11,14,15,35} Because of much lower barrier, the reaction path through α -TS1 is most likely to dominate the reaction. Arrhenius activation energy (1.72 kcal/mol) estimated from the experimentally measured²⁰ rate constants in temperature range of 294–800 K is in very good agreement to our QCISD(T) barrier height (2.03 kcal/mol) for the reaction path R1. The entropies of activation are almost similar at the (U)HF and (U)MP2 level. It was shown for the hydrogen abstraction reaction from chloroethane that the entropies of activation obtained at the (U)MP2 level agrees quite well with the experimental value.¹⁴

The BSSE in the calculated activation energies at the MP2 and QCISD(T) levels are given in Table 7. The BSSE is found to be quite large and varies in between 4.5 and 5.6 kcal/mol. The magnitude of BSSE does not change significantly when one goes from the MP2 to the QCISD(T) method. The BSSE corrected barrier height is found to be widely off from the corresponding experimental value. Similar observation was made earlier by Sekusak and Sabljic for the reaction between haloethanes and OH radical.²⁶

The calculated values of enthalpy change and entropy change for the reactions R1 and R2 are given in Table 8. There is a significant variation in the calculated reaction enthalpies, $\Delta H(298\text{ K})$, with values ranging from -5.78 kcal/mol at the (U)HF/6-311G(d,p) to -19.86 kcal/mol at the (U)MP2/6-311G(d,p) for the reaction R1 and from -1.62 kcal/mol at the (U)HF/6-311G(d,p) to -13.25 kcal/mol at the (U)MP2/6-311G(d,p) for the reaction R2. $\Delta H(298\text{ K})$ values calculated from the QCISD(T)/6-311G(d,p) results are nearly 2.5 kcal/mol lower than the corresponding (U)MP2 values. Since spin projection corrections are fairly small for the reactants and products, PMP2 results are found to be quite close to the (U)MP2 values. The MP2 and QCISD(T) ΔH values calculated for the reaction R1 are in excellent agreement with the experimental value of -18.4 ± 2.4 kcal/mol.³⁶ Since CH_2CHCl_2 radical is substantially higher

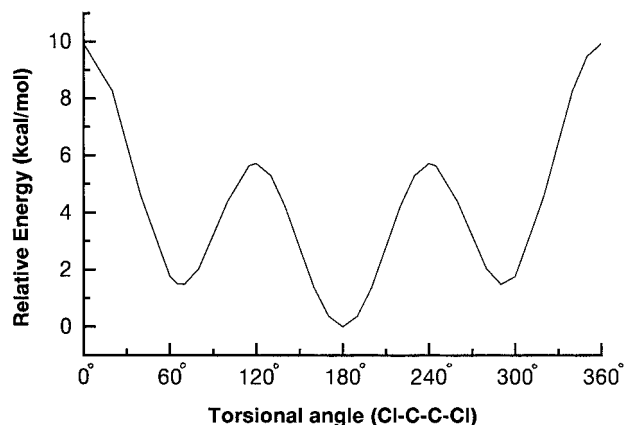
in energy than CH_3CCl_2 radical (by almost 7 kcal/mol at the UMP2 level), the $-\Delta H(298\text{ K})$ for the reaction R2 is smaller than that for the reaction R1. The entropy of reaction ($\Delta S(298\text{ K})$) calculated at the MP2 level for the reaction R1 is also in good agreement with the value estimated from the experimental thermochemical data, $4.8\text{ cal mol}^{-1}\text{ K}^{-1}$ vs $3.8 \pm 1.2\text{ cal mol}^{-1}\text{ K}^{-1}$.³⁶

B. 1,2-Dichloroethane (Reaction R3). Total energies, ZPVEs, and entropies at various levels of theories for both *trans* and *gauche* form of 1,2-DCE and haloethyl radical (CH_2CICHCl) involved in the reaction R3 are reported in Table S5 as Supporting Information. Figure 6 displays relative energies (taking the sum of the energies of *trans*-1,2-DCE and OH radical as zero) of the reactants, TSs, and products at the QCISD(T)/6-311G(d,p) level. At all the levels of theory, the energy of *trans* 1,2-DCE is found to be lower than that of 1,1-DCE. This is opposite to what has been observed in the case of fluorinated ethanes, where the energy of 1,1-difluoroethane is found to be significantly lower than that of 1,2-difluoroethane.¹¹ It was predicted from the spectroscopic observation that the *trans* 1,2-DCE should be about 1.2 kcal/mol more stable than the *gauche* conformer.³⁷ Figure 7 shows the computed potential energy surface connecting the two conformers of 1,2-DCE. At MP2 level the energy difference between the *trans* and *gauche* conformer of 1,2-DCE is found to be 1.47 kcal/mol, whereas the difference amounts to 1.54 kcal/mol at the QCISD(T) level of theory. The barrier heights for going from *trans* to *gauche* and from *gauche* to *trans* configuration are 5.36 kcal/mol (5.05 kcal/mol) and 3.97 kcal/mol (3.59 kcal/mol), respectively, at the MP2 (QCISD(T)) levels of theory. Meanwhile, only one configuration needs to be considered for the product radical, since C-C single bond rotation is almost free in 1,2-dichloroethyl radical, CH_2CICHCl .

Classical barrier heights, ΔE_0^\ddagger , associated with different reaction channels of reaction R3 are given in Table 6. Although four hydrogen atoms are equivalent in *trans* 1,2-DCE, difference in intramolecular interaction gives two distinct TSs, T-TS4 and T-TS5. The additional hydrogen bonding interaction lowers the energy of T-TS4 by more than 1 kcal/mol than the energy of T-TS5 (see Figure 6). Two different TSs have also been found for the hydrogen abstraction from the *gauche* conformer of 1,2-DCE. At the UHF level, G-TS7 is almost 0.8 kcal/mol lower in energy than G-TS6. However, at the MP2 or PMP2 level of calculations, G-TS6 becomes slightly more stable than G-TS7 (see Table 6). This is probably due to the presence of intramolecular hydrogen bonding interaction, which is well represented only at correlated level of theory. Barrier height for the hydrogen abstraction from the α -carbon atom of 1,1-DCE (R1) is nearly 1 kcal/mol lower than the lowest barrier height found for the hydrogen abstraction from 1,2-DCE. This is consistent with the experimental observation that Cl-substitution increases the reactivity at α -position and also to the fact that 1,1-DCE has larger rate coefficient (normalized to the number of abstractable α -H atoms) than 1,2-DCE (2.60×10^{-13} vs $2.20 \times 10^{-13}\text{ cm}^3\text{ molecule}^{-1}\text{ s}^{-1}$) at 296 K.¹⁸ Arrhenius fitting to the experimentally measured rate constants in the temperature range of 292–696 K¹⁹ gives an activation energy of 2.46 kcal/mol, which is nearly 0.6 kcal/mol lower than the lowest barrier height calculated at the QCISD(T) level of theory. The BSSE for the barrier heights were estimated by the CP method²⁷ and are presented in Table 7. Once again the BSSE is found to be unusually large and the BSSE corrected barrier heights become widely off from the available experimental values.

TABLE 8: Heats of Reaction [$\Delta H_0(298\text{ K})$ in kcal/mol] and Entropy of Reaction [$\Delta S_0(298\text{ K})$ in cal mol⁻¹ K⁻¹] Obtained from Various Levels of Calculations with 6-311G(d,p) Basis Set

reaction	$-\Delta H_0(298\text{ K})$				$\Delta S_0(298\text{ K})$		
	HF	MP2(PMP2)	QCISD(T)	exptl ^a	HF	MP2	exptl
CH ₃ CHCl ₂ +OH(R1)	5.8	19.9(20.3)	17.3	18.4 ± 2.4	4.8	4.8	3.8 ± 1.2
CHCl ₂ CH ₃ +OH(R2)	1.6	13.2(13.7)	10.4	4.9	5.3		
CH ₂ ClCH ₂ Cl+OH(R3) (<i>trans</i>)	3.5	17.6(18.3)	15.2	5.9	6.1		
CH ₂ ClCH ₂ Cl+OH(R3) (<i>gauche</i>)	5.2	18.9(19.6)	16.5	6.1	6.3		

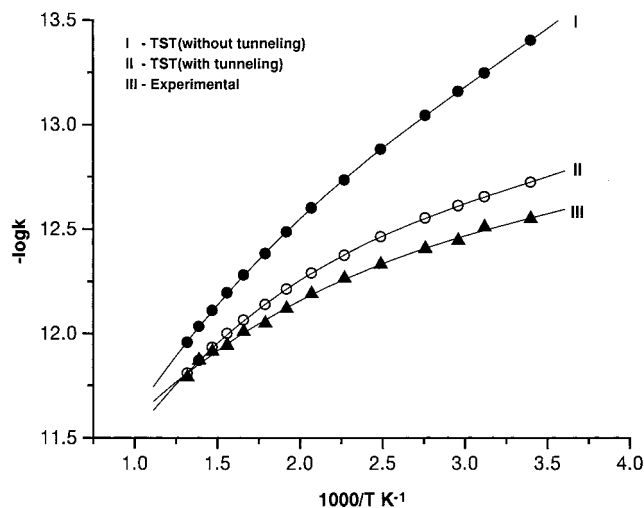
^a Reference 36.**Figure 7.** Torsional potential function for 1,2-dichloroethane as calculated from the MP2=full/6-311G(d,p) results. Energies are calculated relative to the energy of the *trans* conformer.

The enthalpy and entropy change for this reaction, R3, are given in Table 8. Reaction R3 is found to be less exoergic than the reaction R1. Thus reactions are more exoergic when both chlorines are on the same carbon (CH₃CHCl₂) rather than when one chlorine on each carbon (CH₂ClCH₂Cl). This observation corroborates with the suggestion by Evans and Polanyi.³⁸ They suggested that barrier height for exoergic atom abstraction reactions should be proportional to the reaction enthalpy when the central atom remains the same. The barrier height for the reaction R1 is found to be lower than that for the reaction R3. Moreover, in accord with the suggestions of Evans and Polanyi, the barrier height for hydrogen abstraction from the *gauche* conformer is lower than that from the *trans* conformer. The reaction from the *gauche* conformer is found to be slightly more exoergic, since *gauche* 1,2-DCE is higher in energy than the *trans* 1,2-DCE.

3. Rate Constants. Rate constants for the hydrogen abstraction from 1,1- and 1,2-dichloroethane were evaluated using the standard TST expression:³⁹

$$k_{\text{TST}} = \Gamma \frac{k_{\text{B}}T}{h} \frac{Q_{\text{TS}}}{Q_{\text{A}}Q_{\text{B}}} e^{-\Delta E_0^\ddagger/RT}$$

where ΔE_0^\ddagger is the barrier height, Q 's are the respective partition functions, and Γ is a tunneling factor. The classical barrier heights calculated at the QCISD(T)/6-311G(d,p)//(U)MP2=full/6-311G(d,p) level were used for the TST calculations. The electronic partition function of the OH radical was evaluated by taking into account the splitting of 139.7 cm⁻¹ in the ²Π ground state.⁴ The vibrational partition functions were evaluated with the quantum harmonic approximation using the frequencies calculated at the (U)MP2=full/6-311G(d,p) level. However, the internal rotations with low frequencies were treated as a free rotator: the corresponding partition functions were replaced by the partition functions of free rotators. The tunneling correction was performed by following the procedure of Eckart's unsymmetric barrier method.⁴¹

**Figure 8.** Arrhenius plot of the calculated and experimental rate constants (in cm³ molecule⁻¹ s⁻¹) for the hydrogen abstraction reaction between 1,1-dichloroethane and OH radical.

A. 1,1-Dichloroethane (Reactions R1 and R2). The C–C bond rotations in 1,1-DCE and in the transition structures were treated harmonically, since the frequencies associated with these rotations were found to be large: 294, 282, 405, and 404 cm⁻¹ for CH₃CHCl₂, α-TS1, β-TS2, and β-TS3, respectively. The harmonic frequency for the internal rotation of the OH radical in α-TS1 is rather low (71 cm⁻¹) and was treated as a free rotator. In β-TS2 and β-TS3, OH internal rotation frequencies are found to be large (229 and 165 cm⁻¹, respectively) and were treated harmonically. The total rate constant is the sum of the rate constants associated to the three channels (α-TS1, β-TS2, and β-TS3). However, since the barrier height for the reaction R1 is sufficiently lower than those of reaction R2, the total rate constant is nearly equal to the rate constant of reaction R1. The rate constant for the reaction R1 is more than two order of magnitude larger than the rate constant for the reaction R2. For example, the rate constants for the reactions R1 and two channels for R2 are 1.88 × 10⁻¹³, 8.74 × 10⁻¹⁶, and 3.45 × 10⁻¹⁶ cm³ molecule⁻¹ s⁻¹, respectively, at 294 K. Thus, it is most likely that hydrogen atom is abstracted almost exclusively from the α-carbon atom of 1,1-DCE. Namely, not the reaction path R2, but the reaction path R1 through α-TS1 should be a major reaction channel for the reaction of 1,1-DCE.

Figure 8 shows Arrhenius plot of the experimental and calculated rate constants. The rate constants are slightly underestimated by the present TST calculations. The ratio $k_{\text{TST}}/k_{\text{expt}}$ at 294, 521, and 800 K are found to be 0.67, 0.80, and 0.91, respectively. At higher temperature the agreement between the calculated and experimental rate constants is very good. The difference between the calculated and experimental results is larger in lower temperature region, which may arise from the underestimation of the tunneling correction by the Eckart method. The observed non-Arrhenius behaviour of the rate constant may arise from the tunneling effects.

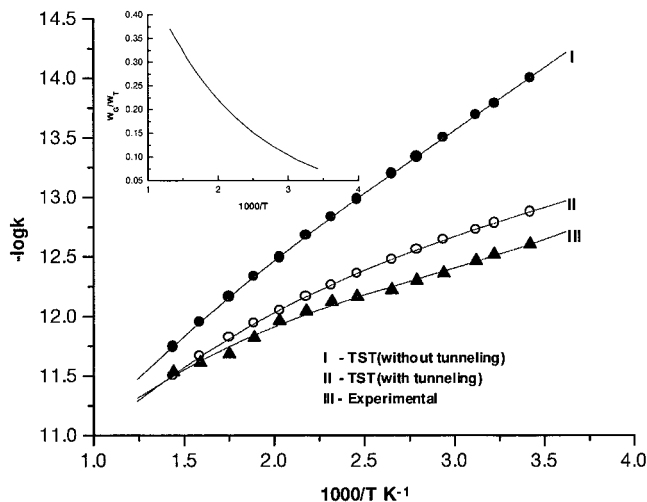


Figure 9. Arrhenius plot of the calculated and experimental rate constants (in $\text{cm}^3 \text{molecule}^{-1} \text{s}^{-1}$) for the hydrogen abstraction reaction between 1,2-dichloroethane and OH radical.

B. 1,2-Dichloroethane (Reaction R3). As discussed earlier, due to the presence of two conformers of 1,2-DCE and four competitive reaction channels, this reaction is more complex than that of 1,1-DCE. The total rate constant can be estimated from the following expression:

$$k_{\text{TST}} = w_{\text{T}}k_{\text{T}} + w_{\text{G}}k_{\text{G}}$$

where w_i 's are the weight factors of each conformer estimated from Boltzmann distribution and k_{T} and k_{G} are the rate constants for the hydrogen abstractions from the *trans* and *gauche* conformers of 1,2-DCE, respectively. k_{T} and k_{G} are the sum of two rate constants associated with two reaction channels of each conformer. Since harmonic frequencies for the C–C single-bond rotation in 1,2-DCE and in the transition structures were found to be low (between 105 to 147 cm^{-1}), this internal motion was treated as a free rotor. Similarly, internal rotations of the OH group in T-TS5 and G-TS7 were treated as a free rotor around the C–H_a bond, since the harmonic frequencies for this rotational motion were found to be low, 156 and 134 cm^{-1} , respectively. Due to the intramolecular hydrogen bonding interaction, the harmonic frequencies for the internal rotation of the OH radical in T-TS4 (227 cm^{-1}) and G-TS6 (238 cm^{-1}) are rather high and, thus, were treated harmonically.

Figure 9 displays Arrhenius plot of the experimentally measured and the calculated rate constants for the reaction R3. The present TST calculations underestimate the rate constants, but the deviation from the experimental values is less than one-order after the tunneling corrections. The deviation is larger in the lower temperature region. For example, at 292 K k_{TST} accounts for 38% of k_{expt} , whereas at 796 K k_{TST} amounts to 65% of k_{expt} . As seen for the reaction of 1,1-DCE, the evaluation of tunneling effects by the Eckart method may not be accurate enough.

The magnitude of the contribution of each reaction channel to the whole reaction rate of R3 varies significantly as the reaction temperature changes. At lower temperature, hydrogen abstraction from *trans* conformer of 1,2-DCE is expected to dominate the reaction because the *trans* conformer is lower in energy than the *gauche* conformer. However, the population of the *gauche* conformer increases as the temperature becomes higher (see the inset of Figure 9). Moreover, the barrier heights for hydrogen abstraction from the *gauche* conformer are lower than those from the *trans* conformer. Thus, in higher temperature

region, the reaction channels not only from the *trans* conformer but also from the *gauche* conformer will significantly contribute to the whole reaction rate of hydrogen abstraction from 1,2-DCE.

As Taylor et al.¹⁹ pointed out, multiple reaction channels in the reaction R3 and the temperature dependence of their contribution to the whole reaction rate partially explains the non-Arrhenius behavior of the rate constants (see III in Figure 9). However, Figure 9 suggests that the non-Arrhenius behavior is also due to the effect of tunneling.

Summary and Conclusions

The stationary points along the reaction coordinates for the hydrogen abstraction by OH radical from 1,1-DCE and 1,2-DCE were located at the (U)HF/6-311G(d,p) and (U)MP2/6-311G(d,p) levels of theory. These reactions were calculated to be exoergic, which is supported by the experimental data as well. Consistent with the suggestion by Evans and Polanyi,³⁸ the calculated barrier heights were found to increase when the exoergicity of the reaction decrease. The optimized geometrical parameters suggested early transition states, in accord with Hammond's postulate. In addition, in some TSs for particular reaction channels, a hydrogen-bonding interaction was suggested between hydrogen atom of incoming OH radical and a chlorine atom. Such hydrogen bonding interactions in the TSs were reflected in the frequencies associated with the rotational motion of OH radical and also in the calculated values for the entropy terms. The analysis based on the transition state theory suggested that experimentally observed non-Arrhenius behavior of the rate constants should be attributed not only to the availability of multiple reaction channels¹⁹ but also to the tunneling effect.

For the hydrogen abstraction from 1,1-DCE, three reaction channels were identified: hydrogen abstraction from α -position via α -TS1 and from β -position via β -TS2 and β -TS3. Hydrogen bonding interactions between OH radical and a chlorine atom were observed in the latter two TSs. However, the barrier height was significantly lower for α -TS1 than for β -TS2 and β -TS3. This is mainly due to the difference in C–H bond energy between α - and β -positions. Thus hydrogen abstraction from α -position via α -TS1 is most likely to be a major reaction channel for 1,1-DCE. The calculated rate constant for hydrogen abstraction from β -position was substantially lower than the value for that from α -position: the difference in rate constant for hydrogen abstraction from α - and β -positions was larger than two order of magnitude. Agreement between the experimentally measured and the calculated rate constants was quite reasonable. The values of heat of reaction (ΔH_{o}) and entropy of reaction calculated for the reaction channel via α -TS1 were in reasonable agreement with the experimentally measured values.³⁶

1,2-DCE has two distinct conformers. In accord with the experimental observation,³² the *trans* conformer was found to be lower in energy by about 1.5 kcal/mol than the *gauche* conformer. The barrier height for going from the former to the latter conformer was calculated to be around 5 kcal/mol. For the hydrogen abstraction reactions of 1,2-DCE, four TSs (T-TS4, T-TS5, G-TS6, and G-TS7) were located and, thus, four reaction channels, two for each conformer, were identified. The hydrogen-bonding interaction between OH radical moiety and a chlorine atom was observed in the two TSs (T-TS4 and G-TS6). In the lower temperature region, the population of the *gauche* conformer would be negligible. Thus, hydrogen abstraction from the *trans* conformer should dominate the reaction at lower temperature. The barrier heights for hydrogen abstraction were found to be lower for the *gauche* conformer than for the

trans conformer. Thus, in higher temperature region, the magnitude of the contribution of the reaction channels originating from the *gauche* conformer of 1,2-DCE should become almost comparable to that of the reaction channels of the *trans* conformer.

Acknowledgment. AKC gratefully acknowledges Drs. J. Tyrrell (USA) and R. Sumathy (Germany) for many useful discussions during the course of this work. Thanks are also due to the New Energy and Industrial Technology Development Organization, Japan, for financial support.

Supporting Information Available: Tables of vibrational frequencies (Tables S1–S3) and of total energies, ZPVEs, and entropies (Tables S4 and S5) calculated for each stationary point. Supporting Information is available free of charge via the Internet at <http://pubs.acs.org>.

References and Notes

- (1) Tuck, R.; Plumb, A.; Condon, E. *Geophys. Res. Lett.* **1990**, *17*, 313. Rosswall, T. *Environ. Sci. Technol.* **1991**, *25*, 567.
- (2) Manzer, L. *Science* **1990**, *249*, 31. Atkinson, R. *Chem. Rev. (Washington, D.C.)* **1986**, *86*, 69. Atkinson, R. *J. Phys. Chem. Ref. Data* **1994**, Monogr. 2.
- (3) Talukdar, R. K.; Mellouki, A.; Gierczak, T.; Burkholder, J. B.; McKeen, S. A.; Ravishankara, A. R. *J. Phys. Chem.* **1991**, *95*, 5815. Ravishankara, A. R.; Turnipseed, A. A.; Jensen, N. R.; Barone, S.; Mills, M.; Howard, C. J.; Solomon, S. *Science* **1994**, *263*, 71.
- (4) Dorigo, A. E.; Houk, K. N. *J. Org. Chem.* **1988**, *53*, 1650.
- (5) Gonzales, C.; McDouall, J. J. W.; Schlegel, H. B. *J. Phys. Chem.* **1990**, *94*, 7467.
- (6) Truong, T. N.; Truhlar, D. G. *J. Chem. Phys.* **1990**, *93*, 1761.
- (7) Francisco, J. S. *J. Chem. Phys.* **1992**, *96*, 7597.
- (8) McKee, M. L. *J. Phys. Chem.* **1993**, *97*, 10971.
- (9) Rayez, M.-T.; Rayez, J.-C.; Berces, T.; Lendvay, J. *J. Phys. Chem.* **1993**, *97*, 5570.
- (10) Melissas, V. S.; Truhlar, D. G. *J. Phys. Chem.* **1994**, *98*, 875.
- (11) Martell, J. M.; Boyd, R. J. *J. Phys. Chem.* **1995**, *99*, 13402.
- (12) Fu, Y.; Lewis-Bevan, W.; Tyrrell, J. *J. Phys. Chem.* **1995**, *99*, 630.
- (13) Sekusak, S.; Gusten, H.; Sabljic, A. *J. Phys. Chem.* **1996**, *100*, 6212.
- (14) Sekusak, S.; Liedl, K. R.; Rode, B. M.; Sabljic, A. *J. Phys. Chem. A* **1997**, *101*, 4245.
- (15) Korchowicz, J.; Kawahara, S.; Matsumura, K.; Uchimaru, T.; Sugie, M. *J. Phys. Chem. A* **1999**, *103*, 3548.
- (16) Schwartz, M.; Marshall, P.; Berry, R. J.; Ehlers, C. J.; Petersson, G. A. *J. Phys. Chem. A* **1998**, *102*, 10074.
- (17) Pedersen, P. S.; Ingversen, J.; Nielsen, T.; Larsen, E. *Environ. Sci. Technol.* **1980**, *14*, 71. Atkinson, R.; Aschmann, S. M.; Pitts, J. N. *Environ. Sci. Technol.* **1984**, *18*, 110.
- (18) Howard, C. J.; Evenson, K. M. *J. Chem. Phys.* **1976**, *64*, 4303.
- (19) Taylor, P. H.; McCarron, S.; Dellinger, B. *Chem. Phys. Lett.* **1991**, *177*, 27.
- (20) Jiang, Z.; Taylor, P. H.; Dellinger, B. *J. Phys. Chem.* **1992**, *96*, 8964.
- (21) Scott, A. P.; Radom, L. *J. Phys. Chem.* **1996**, *100*, 16502.
- (22) Frisch, M. J.; Trucks, G. W.; Schlegel, H. B.; Gill, P. M. W.; Johnson, B. G.; Robb, M. A.; Cheeseman, J. R.; Keith, T.; Petersson, G. A.; Montgomery, J. A.; Raghavachari, K.; Al-Laham, M. A.; Zakrzewski, V. G.; Ortiz, J. V.; Foresman, J. B.; Cioslowski, J.; Stefanov, B. B.; Nanayakkara, A.; Challacombe, M.; Peng, C. Y.; Ayala, P. W.; Chen, W.; Wong, M. W.; Andres, J. L.; Replogle, E. S.; Gomperts, R.; Martin, R. L.; Fox, D. J.; Binkley, J. S.; DeFrees, D. J.; Baker, J.; Stewart, J. P.; Head-Gordon, M.; Gonzalez, C.; Pople, J. A. *Gaussian-94*, Revision D. 3; Gaussian, Inc.: Pittsburgh, PA, 1995.
- (23) Chalasinski, G.; Szczesniak, M. M. *Chem. Rev.* **1994**, *94*, 1723.
- (24) Kestner, N. R. and Combariza, J. E. In *Reviews in Computational Chemistry*, Lipkowitz, K. B., Boyd, D. B., Eds.; John Wiley and Sons, Inc.: New York, 1999; Vol. 13.
- (25) Abkowitz, A. J.; Latajka, Z.; Scheiner, S.; Chalasinski, G. *J. Mol. Struct. (Theochem)* **1995**, *342*, 153.
- (26) Sekusak, S.; Sabljic, A. *J. Comput. Chem.* **1997**, *18*, 1190.
- (27) Boys, S. F.; Bernardi, F. *Mol. Phys.* **1970**, *19*, 553.
- (28) Sekusak, S.; Gusten, H.; Sabljic, A. *J. Chem. Phys.* **1995**, *102*, 7504.
- (29) Levine, R. D. *Physical Chemistry*, 3rd ed.; McGraw-Hill: New York, 1988; p 864.
- (30) Hammond, G. S. *J. Am. Chem. Soc.* **1955**, *77*, 334.
- (31) Dobbs, K. D.; Dixon, D. A.; Komornicki, A. *J. Chem. Phys.* **1993**, *98*, 8852.
- (32) Herzberg, G. *Molecular Spectra and Molecular Structure II. Infrared and Raman Spectra of Polyatomic Molecules*; Van Nostrand: Toronto, 1968.
- (33) Gonzales, C.; Sosa, C.; Schlegel, H. B. *J. Phys. Chem.* **1989**, *93*, 2435.
- (34) Pacey, P. D. *J. Chem. Educ.* **1981**, *58*, 613.
- (35) Martell, J. M.; Mehta, A. K.; Pacey, P. D.; Boyd, R. J. *J. Phys. Chem.* **1995**, *99*, 8661.
- (36) Cohen, N.; Westberg, K. R. *J. Phys. Chem. Ref. Data* **1991**, *20*, 1211.
- (37) Ingold, C. K. *Structure and Mechanism in Organic Chemistry*; Cornell University Press: New York, 1953; p 55.
- (38) Evans, M. G.; Polanyi, M. *Trans. Faraday Soc.* **1938**, *34*, 11.
- (39) Eyring, H. *J. Chem. Phys.* **1935**, *35*, 107.
- (40) Chase, M. W., Jr.; Davies, C. A.; Downey, J. R., Jr.; Frurip, D. J.; McDonald, R. A.; Syverud, A. N. *JANAF Thermochemical Tables*, 3rd ed.; *J. Phys. Chem. Ref. Data* 1985, *14* (Suppl. 1).
- (41) Johnston, H. S.; Heicklen, J. *J. Phys. Chem.* **1962**, *66*, 532.
- (42) Lide, D. R., Ed. *CRC Handbook of Chemistry and Physics*, 78th ed.; CRC Press: Boca Raton, NY, 1997–1998; pp 9–30.
- (43) Shimanouchi, T., Ed. *Tables of Molecular Vibrational Frequencies Consolidated*; National Standard Reference Data Series, National Bureau of Standards: Washington, DC, 1972; Vol. 34, pp 97, 98.